JACS
JOURNAL OF THE AMERICAN CHEMICAL SOCIETY
Communication
pubs.acs.org/JACS

Two-Step Design of a Single-Doped White Phosphor with High Color Rendering

Romain Gautier,*[,†] Xueyan Li,[†] Zhiguo Xia,*[,‡] and Florian Massuyeau[†]

[†]Institut des Matériaux Jean Rouxel (IMN), Université de Nantes, 2 rue de la Houssinière, BP 32229, 44322 Nantes cedex 3, France
[‡]Beijing Municipal Key Lab for Advanced Energy Materials and Technologies, School of Materials Sciences and Engineering, University of Science and Technology Beijing, Beijing 100083, China

Supporting Information

ABSTRACT: A strategy to design step by step an inorganic single-doped white phosphor is demonstrated. The method consists in tuning different contributions of the emission by successively controlling the chemical compositions of the solid solution or nanosegregated host matrix and the oxidation states of the single dopant. We use this approach to design a white phosphor $Na_4CaMgSc_4Si_{10}O_{30}$:Eu with excellent color rendering (CRI > 90) that is similar to common mixed-phosphor light sources but for a single-phase. We show that this methodology can also be extended to other phosphors for use in diverse applications such as biomedicine or telecommunications.

Solid-state lighting (SSL) has recently emerged owing to its ability to replace inefficient traditional incandescent and fluorescent lighting sources. SSL is focusing the researchers' and industrials' attentions because of its fast growing market, estimated to progress from 45% to 70% by 2020.[1] The energy consumed for lighting is expected to be reduced by 40% corresponding to a saving of 640 million tons of CO_2 per year. To date, no other electricity consumer has been reported to have such potential of energy-savings. To produce white LEDs, two main methods are used: (i) LEDs coated with a single phosphor such as blue InGaN LED coated with yellow phosphor YAG:Ce^{3+} or, (ii) LEDs coated with a mixture of phosphors such as UV LEDs coated with blue, green and red phosphors. However, these techniques show different drawbacks: the color rendering of the combination LED + single phosphor is low mainly because of the low contribution in the red spectral region while the mixed phosphors have different aging rates leading to an inappropriate emission color with time.

In this context, a remaining challenge is to discover a single-phased white emitting phosphor with high color rendering to overcome the problem of YAG:Ce^{3+} which is widely used in white LED technologies. This goal is, however, difficult to achieve because exploratory synthesis is commonly time-consuming and repetitive as extremely small modifications in the synthesis of these materials have drastic effects on their photoluminescence properties, and no reliable theory to predict phosphors has been reported to date. Thus, the combination of multidopants in a single host matrix to target multiemission bands has been shown to be interesting to obtain white phosphors; however, the energy transfer (ET) efficiencies are relatively low, and the ET mechanisms between the dopants are also difficult to predict.[2−10] Another interesting method consists of selecting host matrices that exhibit multiple crystallographic sites for a single dopant in order to obtain the superposition of multiple emission spectra.[11] However, the substitution of all sites is not guaranteed and the multiemission bands might not lead to a white phosphor.

A commonly reported approach to tune finely the photoluminescence properties is to modify the composition of the host matrix. Thus, solid solutions are often reported in order to modify the environment of the luminescent centers and consequently tune the properties. However, this control is limited because only one parameter can be modified. This limitation can be visualized on the CIE diagrams because the CIE coordinates of the possible phosphors are always plotted along lines.[12−18] To have more degrees of freedom with the aim of targeting a specific photoluminescence color on the CIE diagram, it is important to include a second parameter that could be finely tuned. In our methodology, we suggest to include the tuning of the oxidation states of the dopants. Hence, the approach consists in mixing different contributions of the emission by tuning two parameters: (a) the composition of the solid solution or nanosegregated host matrix and (b) the oxidation state of the single dopant. As a multitude of doped systems exhibit different emissions when the matrix and the oxidation states of the dopant are different, we postulate the method could be applied to many different systems in order to design white phosphors using a single-dopant.

For a solid solution or nanosegregated $A_xB_{(1-x)}$ doped with D (transition metal, rare earth metal, ...) such as $A_xB_{(1-x)}$:yD^{m+}/$(1-y)D^{n+}$ ($n > m$) and considering a linear evolution of the emission spectra with the contributions of the phosphor centers in different matrices, ET is not expected between dopants present in different oxidation states and between dopants in different environments. Quenching via a metal-to-metal charge transfer state will quench the luminescence and prevent efficient energy transfer as is the case of the Eu^{2+}−Eu^{3+} couple.[19,20]

Therefore, the spectrum could be fitted with the following function:

Received: December 7, 2016
Published: January 18, 2017

DOI: 10.1021/jacs.6b12597
J. Am. Chem. Soc. 2017, 139, 1436−1439

$$I = x[yI_{A:D^{m+}} + (1-y)I_{A:D^{n+}}] + (1-x) \times [yI_{B:D^{m+}} + (1-y)I_{B:D^{n+}}]$$

As the tuning of the oxidation states of dopants can only be carried out after the synthesis of the solid solutions or nanosegregated phases, a general method to design a specific phosphor could be summarized as follows (Figure 1): (a) Calculations of the CIE coordinates of the phosphors $A:D^{m+}$, $B:D^{m+}$, $A:D^{n+}$, and $B:D^{n+}$ to delimit, on the CIE diagram, the possible phosphors that could be targeted by this approach, and define the CIE coordinates of the phosphor to target, (b) Draw a line passing by the CIE coordinates of the target and intersecting the two "sections" (corresponding to the oxidized and reduced solid solution or nanosegregated phosphors) with the same fractions, (c) Synthesize the solid solution or nanosegregated phosphors in oxidized (or reduced) state that corresponds to the intersection of the red dotted line with the "sections" on the CIE diagram, and progressively reduce (or oxidize) the phosphors to tune the luminescence along the dotted line toward the target.

In this work, we focused on Eu doped materials because of their interest in SSL such as the commercial $Y_2O_3:Eu^{3+}$ or $BaMgAl_{10}O_{17}:Eu^{2+}$. Owing to 4f−4f transition, materials doped with Eu^{3+} are typically red phosphors.[21−23] For such dopant, the approach is also slightly simplified because $A:D^{n+}$ and $B:D^{n+}$ have the same CIE coordinates (Figure 1a and Figure 2a). To target white color, one may additionally combine blue and green contributions in the emission spectrum. This can be the case, for example, of the isostructural $NaScSi_2O_6:Eu^{2+}$, which exhibits a green/yellow emission, and $CaMgSi_2O_6:Eu^{2+}$, which exhibits a blue emission.[24,25]

Thus, for the $(CaMg)_x(NaSc)_{1-x}Si_2O_6:Eu$ nanosegregated phase, the equation corresponding to the resulting emission spectrum can be written as

$$I = (1-y)I_{CMS:Eu^{3+}} + y[xI_{CMS:Eu^{2+}} + (1-x)I_{NSS:Eu^{2+}}]$$

The emission spectrum is a combination of three different spectra from $(CaMg)Si_2O_6:Eu^{3+}$ (CMS:Eu^{3+}) or $(NaSc)Si_2O_6:Eu^{3+}$ (NSS:Eu^{3+}) corresponding to the red contribution, CMS:Eu^{2+} for the green/yellow contribution, and NSS:Eu^{2+} for

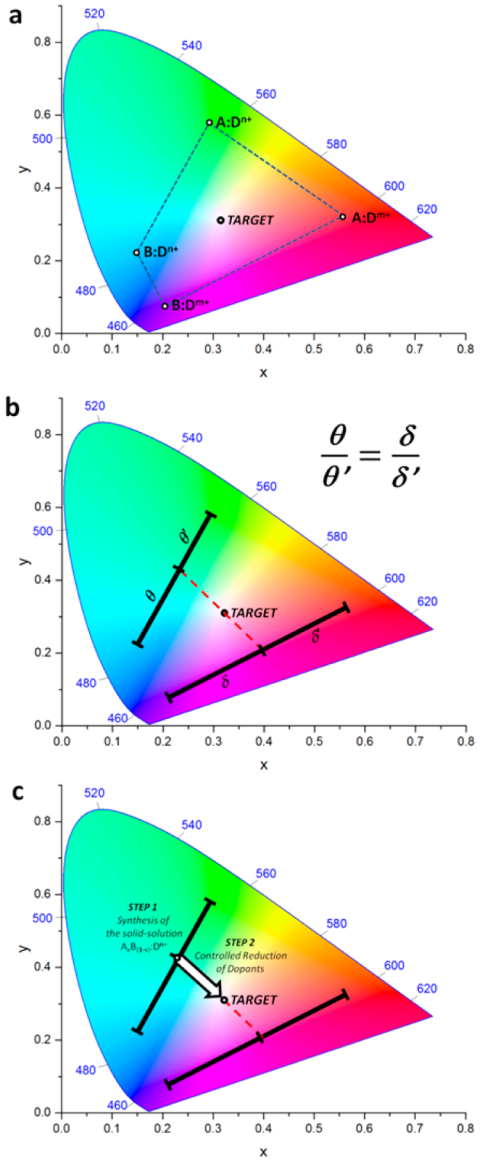

Figure 1. Representation of the approach to design single-doped white phosphor: (a) Determination of CIE coordinates of the phosphors $A:D^{m+}$, $B:D^{m+}$, $A:D^{n+}$, and $B:D^{n+}$ ($n > m$) and the target, (b) Determination of the CIE coordinates which the solid solution or nanosegregated phosphor should have when the dopants are fully oxidized and fully reduced, (c) Step 1: Synthesis of the solid solution or nanosegregated phosphor and Step 2: Controlled reduction of the dopants.

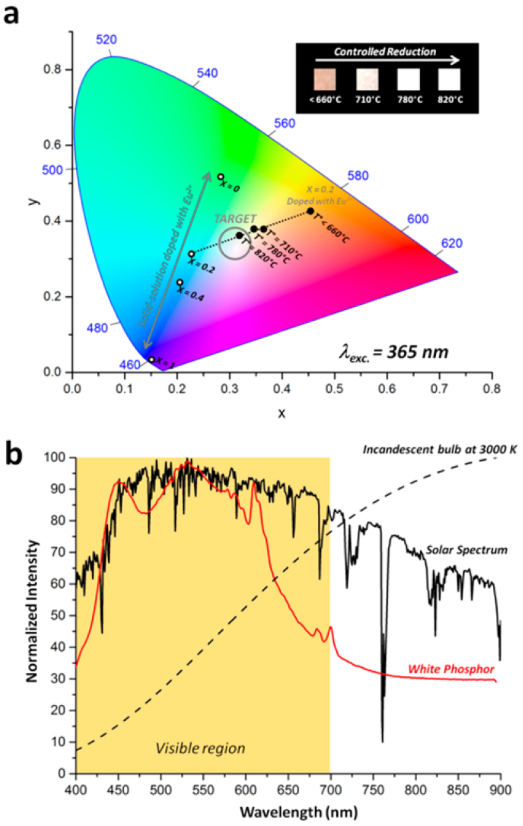

Figure 2. Application of the two-step approach for $(CaMg)_x(NaSc)_{1-x}Si_2O_6:Eu$: (a) Representation of the CIE coordinates for the phase doped with Eu^{2+} (white dots) and for reduction of the dopants Eu^{3+} into Eu^{2+} with $x = 0.2$ (black dots), and (b) emission spectra (excited at 365 nm) of the white phosphor and comparison with solar spectrum.

DOI: 10.1021/jacs.6b12597
J. Am. Chem. Soc. 2017, 139, 1436−1439

the blue contribution. Thus, we used the two-step approach to (i) mix in appropriate amount green and blue contributions by adjusting the value of x and, then, (ii) add a red contribution by modifying the ratio y of Eu^{3+}/Eu^{2+}.

At first, the goal is to mix appropriately two of the three contributions of the emission. In the case of $(CaMg)_x(NaSc)_{1-x}Si_2O_6$:0.03$Eu^{2+}$, phosphors corresponding to x = 0, 0.2, 0.4, and 1 were prepared by sol−gel method.[25] Powder X-ray diffraction was carried out on this series of compounds and the samples were shown to be pure (Figure S1). Room temperature photoluminescence spectra were measured, and the appropriate ratio of green and blue emissions was found for the sample with x = 0.2 (Figure S2). For this material, the CIE coordinate is on a line passing by the CIE coordinate of a white phosphor and the CIE coordinate of the Eu^{3+} doped compounds (Figure 2a).

In the second step, $Na_4CaMgSc_4Si_{10}O_{30}$:0.03$Eu^{2+}$ (corresponding to x = 0.2) has been oxidized into $Na_4CaMgSc_4Si_{10}O_{30}$:0.03$Eu^{3+}$ at 1000 °C for 24 h. A controlled reduction of the dopants Eu^{3+} into Eu^{2+} was then carried out at low temperature. This approach can be compared to the one that consists of using an oxygen getter (such as CaH_2 or Ti) together with the materials in a glass tube sealed under vacuum in order to carry out a topotactic reduction.[26−36] For our materials, we modified this method by using a silica tube under permanent dynamic vacuum in order to reach higher temperatures. This process was carried out by increasing temperature from 600 to 820 °C. Here, the goal is to finely reduce Eu^{3+} dopants responsible of a red contribution into Eu^{2+} responsible of the contributions Green + Blue in appropriate ratio. At 820 °C, the right ratio of R+G+B could be found giving the possibility to obtain a single-doped white phosphor (Figure S3). This process could be followed by plotting the CIE coordinates as shown in Figure 2a.

The spectrum of the resulting white phosphor is comparable to the solar spectrum (Figure 2b). Thus, the correlated color temperature (CCT) is 5868 K, which corresponds to the temperature of sunlight above the atmosphere (about 5900 K). Moreover, the compound has a color rendering index (CRI) of 91. This value is similar to the mixed-phosphor light sources, which have commonly a CRI higher than 90 and well above the CRI of single phased phosphor (commonly <75).[1,37,38]

This design is possible because no energy transfer occurs between the dopants as mentionned above. Recently, Xia et al. showed that the $(CaMg)_x(NaSc)_{1-x}Si_2O_6$:$Eu^{2+}$ phase, which exhibits a quantum efficiency (QE) of about 12%,[24] presented a nanosegregation of isostructural $(CaMg)Si_2O_6$ and $(NaSc)Si_2O_6$ nanodomains with proportional number of Eu ions.[25] For our material, the measured internal QE value of $Na_4CaMgSc_4Si_{10}O_{30}$:0.03Eu phosphor is determined to be 37% under 365 nm excitation. The nanosegregation not only makes the spectral profile to be predictable but also would improve the efficiency because energy transfer between centers and energy lost due to defects would be limited. The improved QE after tuning the oxidation state of the dopant also supports the result showing that ET is not observed between dopants in different oxidation states. This suggests that the step by step strategy to design an inorganic single-doped white phosphor does not only enable the high color rendering but also benefits the photoluminescence QE. Moreover, the temperature dependent luminescence (Figure S4) shows a slow decrease of the intensity with temperature but the spectra at room temperature before and after heating to 200 °C are similar. This result shows that the ratio Eu^{3+}/Eu^{2+} could be kept stable if the phosphor is in conjunction with a near UV diode.

In summary, we showed a two step strategy to target a single-doped white phosphor: (i) tuning the solid solution or nanosegregated host matrix and (ii) tuning the oxidation state of the dopant. The temperatures of synthesis (typically >1000 °C), reduction of dopants (typically 400−900 °C) and use in LEDs (up to 250 °C) are within different ranges. The control of the oxidation states of dopants without modifying the host matrix and the stability of phosphors in devices (no reoxydation of the dopants) are also guaranteed. This approach can be generalized to many different systems doped with lanthanides or transition metals because most of these elements exhibit different oxidation states with specific photoluminescence properties, and host matrices for which the compositions can be tuned are also common. Moreover, the identification of PL colors that could be reached (delimitation on the CIE diagram of the possible phosphors prior to their synthesis) enables the fine optimization of the color rendering of technologically useful phosphors. The methodology, which has been used in this work to target a new white phosphor, could also be of interest to target photoemissions in IR region for applications in telecommunications or biomedicine.

■ ASSOCIATED CONTENT

Supporting Information

The Supporting Information is available free of charge on the ACS Publications website at DOI: 10.1021/jacs.6b12597.

Experimental details, X-ray diffraction patterns, photoluminescence spectra, photoluminescence vs temperature, Figure S1−S4 (PDF)

■ AUTHOR INFORMATION

Corresponding Authors

*Romain.Gautier@cnrs-imn.fr

*xiazg@ustb.edu.cn

ORCID

Romain Gautier: 0000-0002-3042-0335

Notes

The authors declare no competing financial interest.

■ ACKNOWLEDGMENTS

The work in France was supported by the National Agency for Research (ANR Young Researchers, ANR-16-CE08-0003-01, Combi-SSL project). We also thank Fanch Guillou for machining the stumatite and design crucibles for the controlled reduction of dopants. The work in China was supported by the National Natural Science Foundations of China (Grant Nos. 91622125 and 51572023), and Natural Science Foundations of Beijing (2172036).

■ REFERENCES

(1) Pust, P.; Schmidt, P. J.; Schnick, W. *Nat. Mater.* **2015**, *14*, 454.

(2) Yang, W.-J.; Luo, L.; Chen, T.-M.; Wang, N.-S. *Chem. Mater.* **2005**, *17*, 3883.

(3) Yang, W.-J.; Chen, T.-M. *Appl. Phys. Lett.* **2006**, *88*, 101903.

(4) Chang, C.-K.; Chen, T.-M. *Appl. Phys. Lett.* **2007**, *90*, 161901.

(5) Ye, S.; Wang, X.-M.; Jing, X.-P. *J. Electrochem. Soc.* **2008**, *155*, J143.

(6) Zhang, M.; Liang, Y.; Tang, R.; Yu, D.; Tong, M.; Wang, Q.; Zhu, Y.; Wu, X.; Li, G. *RSC Adv.* **2014**, *4*, 40626.

DOI: 10.1021/jacs.6b12597
J. Am. Chem. Soc. 2017, 139, 1436−1439

(7) Chen, Y.; Li, Y.; Wang, J.; Wu, M.; Wang, C. *J. Phys. Chem. C* **2014**, *118*, 12494.
(8) Shang, M.; Li, C.; Lin, J. *Chem. Soc. Rev.* **2014**, *43*, 1372.
(9) Kang, F.; Zhang, Y.; Peng, M. *Inorg. Chem.* **2015**, *54*, 1462.
(10) Liu, L.; Wang, L.; Zhang, C.; Cho, Y.; Dierre, B.; Hirosaki, N.; Sekiguchi, T.; Xie, R.-J. *Inorg. Chem.* **2015**, *54*, 5556.
(11) Hagemann, H.; Bill, H.; Rey, J. M.; Kubel, F.; Calame, L.; Lovy, D. *J. Phys. Chem. C* **2015**, *119*, 141.
(12) Zhang, Q.; Wang, J.; Zhang, M.; Su, Q. *Appl. Phys. B: Lasers Opt.* **2008**, *92*, 195.
(13) Zhang, M.; Wang, J.; Zhang, Z.; Zhang, Q.; Su, Q. *Appl. Phys. B: Lasers Opt.* **2008**, *93*, 829.
(14) Im, W. B.; George, N.; Kurzman, J.; Brinkley, S.; Mikhailovsky, A.; Hu, J.; Chmelka, B. F.; DenBaars, S. P.; Seshadri, R. *Adv. Mater.* **2011**, *23*, 2300.
(15) Denault, K. A.; George, N. C.; Paden, S. R.; Brinkley, S.; Mikhailovsky, A. A.; Neuefeind, J.; DenBaars, S. P.; Seshadri, R. *J. Mater. Chem.* **2012**, *22*, 18204.
(16) Ji, H.; Huang, Z.; Xia, Z.; Molokeev, M. S.; Atuchin, V. V.; Huang, S. *Inorg. Chem.* **2014**, *53*, 11119.
(17) Xia, Z.; Molokeev, M. S.; Im, W. B.; Unithrattil, S.; Liu, Q. *J. Phys. Chem. C* **2015**, *119*, 9488.
(18) Xia, Z.; Ma, C.; Molokeev, M. S.; Liu, Q.; Rickert, K.; Poeppelmeier, K. R. *J. Am. Chem. Soc.* **2015**, *137*, 12494.
(19) Wickleder, C. *Z. Für Naturforschung B* **2014**, *57*, 901.
(20) Setlur, A. A. *Electrochem. Solid-State Lett.* **2012**, *15*, J25.
(21) Xie, M.; Li, Y.; Li, R. *J. Lumin.* **2013**, *136*, 303.
(22) Skaudzius, R.; Katelnikovas, A.; Enseling, D.; Kareiva, A.; Jüstel, T. *J. Lumin.* **2014**, *147*, 290.
(23) Behrh, G. K.; Gautier, R.; Latouche, C.; Jobic, S.; Serier-Brault, H. *Inorg. Chem.* **2016**, *55*, 9144.
(24) Xia, Z.; Zhang, Y.; Molokeev, M. S.; Atuchin, V. V.; Luo, Y. *Sci. Rep.* **2013**, *3*, 3310.
(25) Xia, Z.; Liu, G.; Wen, J.; Mei, Z.; Balasubramanian, M.; Molokeev, M. S.; Peng, L.; Gu, L.; Miller, D. J.; Liu, Q.; Poeppelmeier, K. R. *J. Am. Chem. Soc.* **2016**, *138*, 1158.
(26) Hayward, M. A.; Green, M. A.; Rosseinsky, M. J.; Sloan, J. *J. Am. Chem. Soc.* **1999**, *121*, 8843.
(27) Tsujimoto, Y.; Tassel, C.; Hayashi, N.; Watanabe, T.; Kageyama, H.; Yoshimura, K.; Takano, M.; Ceretti, M.; Ritter, C.; Paulus, W. *Nature* **2007**, *450*, 1062.
(28) Hayward, M. A.; Rosseinsky, M. J. *Nature* **2007**, *450*, 960.
(29) Kageyama, H.; Watanabe, T.; Tsujimoto, Y.; Kitada, A.; Sumida, Y.; Kanamori, K.; Yoshimura, K.; Hayashi, N.; Muranaka, S.; Takano, M.; Ceretti, M.; Paulus, W.; Ritter, C.; André, G. *Angew. Chem.* **2008**, *120*, 5824.
(30) Seddon, J.; Suard, E.; Hayward, M. A. *J. Am. Chem. Soc.* **2010**, *132*, 2802.
(31) Dixon, E.; Hadermann, J.; Ramos, S.; Goodwin, A. L.; Hayward, M. A. *J. Am. Chem. Soc.* **2011**, *133*, 18397.
(32) Romero, F. D.; Coyle, L.; Hayward, M. A. *J. Am. Chem. Soc.* **2012**, *134*, 15946.
(33) Kaur Behrh, G.; Serier-Brault, H.; Jobic, S.; Gautier, R. *Angew. Chem.* **2015**, *127*, 11663.
(34) Liu, B.-M.; Zhang, Z.-G.; Zhang, K.; Kuroiwa, Y.; Moriyoshi, C.; Yu, H.-M.; Li, C.; Zheng, L.-R.; Li, L.-N.; Yang, G.; Zhou, Y.; Fang, Y.-Z.; Hou, J.-S.; Matsushita, Y.; Sun, H.-T. *Angew. Chem.* **2016**, *128*, 5051.
(35) Zhang, K.; Hou, J.-S.; Liu, B.-M.; Zhou, Y.; Yong, Z.-J.; Li, L.-N.; Sun, H.-T.; Fang, Y.-Z. *RSC Adv.* **2016**, *6*, 78396.
(36) Jiang, T.; Li, X.; Bujoli-Doeuff, M.; Gautron, E.; Cario, L.; Jobic, S.; Gautier, R. *Inorg. Chem.* **2016**, *55*, 7729.
(37) Ye, S.; Xiao, F.; Pan, Y. X.; Ma, Y. Y.; Zhang, Q. Y. *Mater. Sci. Eng., R* **2010**, *71*, 1.
(38) Dohner, E. R.; Hoke, E. T.; Karunadasa, H. I. *J. Am. Chem. Soc.* **2014**, *136*, 1718.

DOI: 10.1021/jacs.6b12597
J. Am. Chem. Soc. 2017, 139, 1436−1439